A TRIAL TO CALIBRATE POLARIMETRIC PI-SAR DATA AND ITS IMAGE ANALYSIS

Koji KIMURA, Yoshio YAMAGUCHI, and Hiroyoshi YAMADA
Faculty of Engineering, Niigata University
2-8050, Ikarashi, Niigata 950-2181, Japan
E-mail: kkimu@wave.ie.niigata-u.ac.jp

1. Introduction

PI-SAR (Polarimetric and Interferometric Synthetic Aperture Radar) is developed for the purpose of environmental observation and prevention for disasters by CRL and NASDA. The resolution of image obtained by the radar is 3 meters in the L-band, while 1.5 meters in the X-band. This paper presents classification results of targets on the earth (water, farmland, vegetation, residential areas) using scattering matrix component and 3 fundamental component (representing odd-bounce, even-bounce, and generation of circular polarization) images of the L-band PI-SAR data of Ikarashi site in Niigata City. These data are based on Sinclair scattering matrices of the original PI-SAR images. However, there exist speckle noises in SAR images, multilook processing, which reduces the affect of the noises, is needed for analysis. In addition, since polarimetric calibration is not carried out in the PI-SAR data, we tried to calibrate it. A small area in the sea is extracted as a calibration target in this paper. After multilook and polarimetric calibration processing, the entire image was classified by the maximum-likelihood method using linear, circular polarization and three components as feature vector components. The total classification accuracy was approximately 80 %.

2. Imaged area and classification algorithm

Ikashi area in Niigata City, which is used for analysis, is illustrated in Fig. 1. Niigata University is on the upper right side of this figure.
A lot of house stand closely together around the university. The Sea of Japan is on the top of this figure, while a number of farmlands on the bottom. Pine woods are along the coastline. A small river crosses near the university. Therefore, four classes (water, farmland, vegetation and residential area) are defined. From original fully polarimetric PI-SAR images, linear, circular polarization component and three component images are produced. Each pixel in the image of Ikarashi area is assigned to one of four clusters by averages of each parameter as feature vector components. In this paper, the maximum-likelihood method is used as a classification algorithm. The sample, which is a classification criterion, is extracted from a number of training areas in each cluster, which describes the characteristics of each cluster the best.

Fig. 1 Ikarashi area in Niigata City.

3. Multilook processing

There exist speckle noises in the PI-SAR image, which degrade classification accuracy. Therefore, multilook processing is necessary for reducing the affect of the noises. Since each pixel is assigned to one scattering matrix, the averaging scheme is based on the transformation of scattering matrix into Kennuagh matrix. In this paper, the multilook processing is carried out in 4 × 4 pixels.

4. Polarimetric calibration

Since Scattering matrices measured by PI-SAR contain polarimetric errors, they need polarimetric

calibration.

The errors can be classified into two categories; 1) Co-pol channel imbalance, and 2) X-pol channel imbalance. To remove the errors, calibration targets are used. However, since the polarimetric calibration data is not available at present, we used a small area in the sea as a calibration target (see Fig. 2). If ocean area is nearly flat, the scattering property of the area is similar to that of a plate. Theoretical Sinclair scattering matrix $[\boldsymbol{S}]$ with relative amplitude and phase for a plate is written as

$$[\boldsymbol{S}]_{plate} = \begin{bmatrix} 1 & 0 \\ 0 & 1 \end{bmatrix}. \quad (1)$$

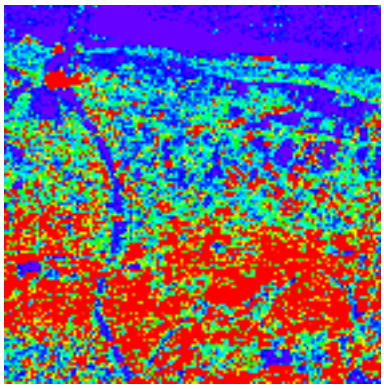

Fig. 2 The calbration target in the sea.

The Co-pol channel imbalance is caused by a difference in antenna pattern in the polarimetric channels. For example, S_{HH} should be equal to S_{VV} for a plate, however, the difference in antenna pattern in the H-pol and V-pol direction causes different amplitude and phase for S_{HH} and S_{VV} in the synthetic aperture processing. This factor can be incorporated into a measured scattering matrix $[\boldsymbol{Z}]$ expressed as

$$[\boldsymbol{Z}] = \begin{bmatrix} Z_{HH} & Z_{VH} \\ Z_{VH} & Z_{VV} \end{bmatrix} = [\boldsymbol{R}][\boldsymbol{S}][\boldsymbol{T}] = \begin{bmatrix} 1 & 0 \\ 0 & f_1 \end{bmatrix} \begin{bmatrix} S_{HH} & S_{VH} \\ S_{VH} & S_{VV} \end{bmatrix} \begin{bmatrix} 1 & 0 \\ 0 & f_1 \end{bmatrix}, \quad (2)$$

where $[\boldsymbol{R}]$ and $[\boldsymbol{T}]$ are matrices containing system error factors on receiver and transmitter, respectively. f_1 is a variable for the Co-pol channel imbalance.

In addition, the X-pol channel imbalance problem needs be considered since there are waves and surges in ocean area and the area is not completely flat. S_{VH} is not strictly equal to zero. If the polarization isolation in the radar system is neglected, the factor to resolve the X-pol channel imbalance can be incorporated into a scattering matrix as

$$\begin{bmatrix} S_{HH} & S_{VH} \\ S_{VH} & S_{VV} \end{bmatrix} \qquad \begin{bmatrix} S_{HH} & f_2 S_{VH} \\ f_2 S_{VH} & S_{VV} \end{bmatrix}. \quad (3)$$

f_2 is a variable for the X-pol channel imbalance. Therefore, the expression for the measured scattering matrix $[\boldsymbol{Z}]$ containing the Co- and X-pol channel imbalance becomes

$$[\boldsymbol{Z}] = \begin{bmatrix} Z_{HH} & Z_{VH} \\ Z_{VH} & Z_{VV} \end{bmatrix} = [\boldsymbol{R}][\boldsymbol{W}][\boldsymbol{T}] = \begin{bmatrix} 1 & 0 \\ 0 & f_1 \end{bmatrix} \begin{bmatrix} S_{HH} & f_2 S_{VH} \\ f_2 S_{VH} & S_{VV} \end{bmatrix} \begin{bmatrix} 1 & 0 \\ 0 & f_1 \end{bmatrix}. \quad (4)$$

It is possible to calibrate measured scattering matrix $[\boldsymbol{Z}]$ by obtaining f_1 and f_2.

For a plate, S_{HH} is equal to S_{VV}, therefore

$$f_1 = \sqrt{\frac{Z_{VV}}{Z_{HH}}}. \quad (5)$$

However, since ocean area is not completely flat, S_{VH} is not strictly equal to zero as a plate. In ocean area, it is expected that the backscattering coefficient for VH is smaller than that for HH and VV. Therefore, the condition for S_{VH} is assumed as

$$\sigma^0_{VH}\,(dB) < \sigma^0_{VV} - 10.0(dB) \quad (6)$$

Under these conditions, we calculated f_1 and f_2 as

$$f_1 = 0.722146 + j1.251282, \quad f_2 = 2.424182 + j1.587961. \quad (7)$$

The validity of (7) is not apparent, but the factor f_1 and f_2 will be used for classification which follows, because there are no evidential calibration data available.

The polarimetric signatures of the extracted area before and after the calibration are illustrated in Fig. 3 (a) and (b), respectively. After the calibration, the signature becomes similar to that of a plate. In addition, the polarimetric signatures of training areas in each class after the calibration are illustrated

in Fig. 4. In this paper, 16 5 × 5 pixels are extracted from each class as training areas. From these signatures, it is seen that the signatures of water and farmland are similar to that of a plate, which is physically true from the polarimetric point of view.

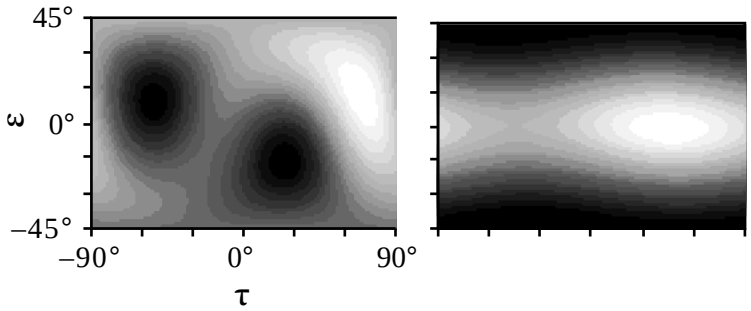

(a) Before calibration. (b) After calibration.

Fig. 3 Polarimetric signatures in the area extracted from the sea.

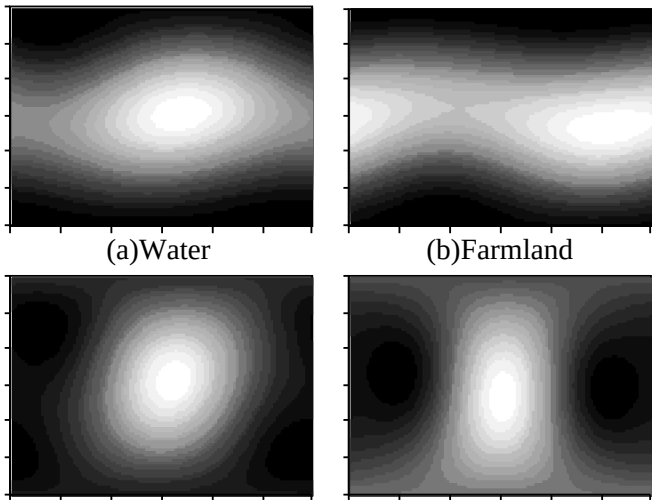

(a)Water (b)Farmland

(c)Vegetation (d)Residential

Fig. 4 Polarimetric signatures of training areas in each class.

5. Classification result

Finally, the classified images and the classification accuracy tables are shown in Fig. 5 and Table 1 using linear, circular polarization and three component images, respectively. In Table 1, "Farm" stands for farmland, "Veg" vegetation and "Resi" residential area, respectively. The diagonal elements show the accuracy of assigning pixels to the exact class. From these tables, it is seen that target classification with high accuracy is possible using any image.

6. Conclusion

In this paper, we have shown analysis results of PI-SAR image of Ikarashi area in Niigata City using multilook and polarimetric calibration. The total classification accuracy is around 80 %, although the accuracy depends on the combination of polarimetric images as HV. The polarimetric calibration on the measured scattering matrix still needs further research.

Acknowledgment

The authors thank CRL and NASDA for providing the PI-SAR data used for analysis. This work in part was supported by Grant in Aid for Scientific Research, Ministry of Education, Japan.

Reference

[1] Y.Yamaguchi, *FUNDAMENTALS OF POLARIMETRIC RADAR AND ITS APPLICATION*, REALIZE INC., pp. 52-74, April 1998.

[2] E. Krogager, Z. H. Czyz, "Properties of the sphere, diplane, helix decomposition," *Proc. of the 3rd International Workshop on Radar Polarimetry*, pp.106-115, 1995.

[3] T. Nagai, et al, "Use of multi-polarimetric enhanced images in SIR-C/X-SAR land-cover classification," *IEICE Trans. Commun*., vol. E-B, no.11, pp.1696-1702, 1997.

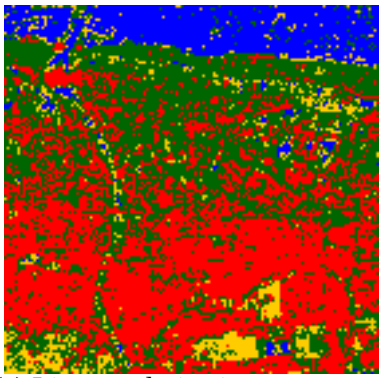

(a) Linear polarization component

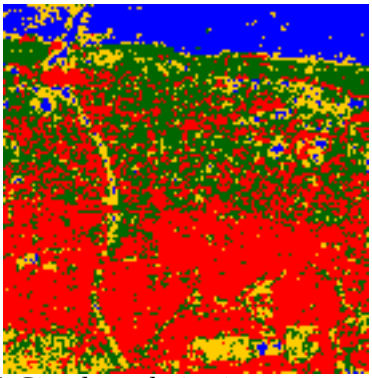

(b) Circular polarization component

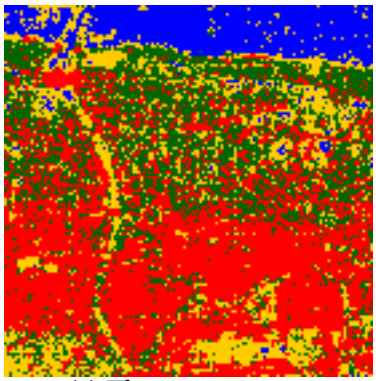

(c) Three component

Fig. 5 Classified images.

Water Farmland
Vegetation Residential

Table 1. Tables of classification accuracy.

(a) Linear polarization component

	Water	Farm	Veg	Resi
Water	95.07	1.86	3.07	0.00
Farm	0.29	70.40	25.92	3.39
Veg	0.13	12.88	85.13	1.86
Resi	0.00	3.38	32.62	64.00

Total=77.19%

(b) Circular polarization component

	Water	Farm	Veg	Resi
Water	97.98	1.82	0.19	0.00
Farm	0.34	77.82	16.49	5.35
Veg	0.14	32.83	65.65	1.39
Resi	0.00	6.86	17.21	75.94

Total=82.92%

(c) Three component

	Water	Farm	Veg	Resi
Water	97.25	2.56	0.19	0.00
Farm	0.34	84.20	10.23	5.23
Veg	0.13	42.09	55.38	2.39
Resi	0.00	16.53	15.64	67.84

Total=79.52%